Transcriptome analyses reveal molecular mechanisms underlying functional recovery after spinal cord injury

Hongmei Duan[a,1], Weihong Ge[b,1], Aifeng Zhang[c,1], Yue Xi[a,1], Zhihua Chen[d,1], Dandan Luo[e], Yin Cheng[b], Kevin S. Fan[f], Steve Horvath[g], Michael V. Sofroniew[h], Liming Cheng[i], Zhaoyang Yang[a,j,2], Yi E. Sun[e,b,2], and Xiaoguang Li[a,j,2]

[a]Department of Biomedical Engineering, School of Biological Science and Medical Engineering, Beihang University, Beijing 100191, China; [b]Department of Psychiatry and Biobehavioral Sciences, David Geffen School of Medicine, University of California Los Angeles, Los Angeles, CA 90095; [c]Beijing Friendship Hospital, Capital Medical University, Beijing 100068, China; [d]Department of Biochemistry and Molecular Biology, Institute of Clinical Medical Sciences, China-Japan Friendship Hospital, Beijing 100029, China; [e]Stem Cell Translational Research Center, Tongji Hospital, Tongji University School of Medicine, Shanghai 200065, China; [f]Department of Computer Engineering, University of California Santa Barbara, Santa Barbara, CA 93106; [g]Department of Human Genetics, David Geffen School of Medicine, University of California Los Angeles, Los Angeles, CA 90095; [h]Department of Neurobiology, David Geffen School of Medicine, University of California Los Angeles, Los Angeles, CA 90095; [i]Department of Spine Surgery, Tongji Hospital, Tongji University School of Medicine, Shanghai 200065, China; and [j]Department of Neurobiology, School of Basic Medical Sciences, Captial Medical University, Beijing 100069, China

Spinal cord injury (SCI) is considered incurable because axonal regeneration in the central nervous system (CNS) is extremely challenging, due to harsh CNS injury environment and weak intrinsic regeneration capability of CNS neurons. We discovered that neurotrophin-3 (NT3)-loaded chitosan provided an excellent microenvironment to facilitate nerve growth, new neurogenesis, and functional recovery of completely transected spinal cord in rats. To acquire mechanistic insight, we conducted a series of comprehensive transcriptome analyses of spinal cord segments at the lesion site, as well as regions immediately rostral and caudal to the lesion, over a period of 90 days after SCI. Using weighted gene coexpression network analysis (WGCNA), we established gene modules/programs corresponding to various pathological events at different times after SCI. These objective measures of gene module expression also revealed that enhanced new neurogenesis and angiogenesis, and reduced inflammatory responses were keys to conferring the effect of NT3-chitosan on regeneration.

NT3 | chitosan | WGCNA | spinal cord injury | transcriptome

Spinal cord injury (SCI) is a debilitating medical condition that often leads to permanent impairment of sensory and motor functions. SCI is considered almost incurable because axons in the central nervous system (CNS), unlike those in the peripheral nervous system (PNS), are believed not to regenerate. The innate ability of mature CNS neurons to regenerate is much weaker than that of PNS neurons (1). In addition, myelin debris in the injured CNS is more inhibitory toward axonal growth compared to that in the PNS (2). Moreover, the mode of immune cell infiltration and microglia activation are different in CNS versus PNS, resulting in a different cellular microenvironment, which crucially influences the outcome, i.e., PNS axons regenerate, while CNS axons do not (3).

Over the years, SCI research has focused on ways to promote the long-distance growth of CNS motor axons, mainly by neutralizing inhibitory myelin components and/or changing the neuronal intrinsic program to enable better regeneration (4). Unfortunately, however, although numerous studies have been carried out following this line of strategy, no major breakthroughs translatable to therapy have been achieved. In recent years, efforts toward promoting long distance axonal growth have been complemented with alternative approaches aimed at using exogenous stem cells to generate local new neurons that form nascent relay neural networks to pass ascending and descending neurotransmission signals with or without long-distance axonal growth (5–7).

SCI is a complex medical condition. The primary lesion includes the physical traumatic wounding of both white and gray matter, breakdown of the vasculature system, and acute immune reactions, which is followed by secondary lesions, such as demyelination, additional immune cell infiltration, inflammation, glial scar formation, impaired neurotransmission, and neuronal

apoptosis (8). Secondary lesions are intermingled with intrinsic repair processes, including remyelination, reestablishment of the vasculature system, reactivation of presumptive endogenous neural stem/progenitor cells (NSCs), and axonal sprouting and growth (9). In the past, these various pathological events have been studied in an isolated or incoherent manner without assembling the factors into a framework to provide a holistic view. One major challenge in the field of SCI research is the huge variability caused not only by different lesion models and animal strains, but also by even subtle changes in the exact lesion operations. Moreover, most analyses for evaluating neural repair/regeneration have been anatomic, behavioral, and sometimes electrophysiological, including extracellular recordings (1, 4, 10, 11). These analyses are relatively low in resolution, and particularly the behavioral assays can be highly variable and subjective to errors in human judgment. As a result, the SCI research field has suffered from substantial inconsistency and irreproducibility of various reported findings, results, and conclusions.

In addition to double-blind designs of behavioral assays proposed as necessary, the development of more objective, quantitative, and

Significance

In this study, we used gene expression analyses to unveil mechanisms underlying NT3-chitosan–induced spinal cord regeneration. Using a powerful bioinformatics tool known as weighted gene coexpression network analysis, we have established gene modules and programs representing various events at different times after spinal cord injury (SCI) and also demonstrated that enhanced new neurogenesis and vascularization, as well as reduced inflammatory responses, are keys to conferring the effect of NT3-chitosan on regeneration. The objectivity of this approach and the use of big data processing have opened a new pathway in SCI research. Such quantitative, objective, and sensitive measures could provide a standardized approach in the future to reveal mechanistic insight into various potential interventions for SCI repair.
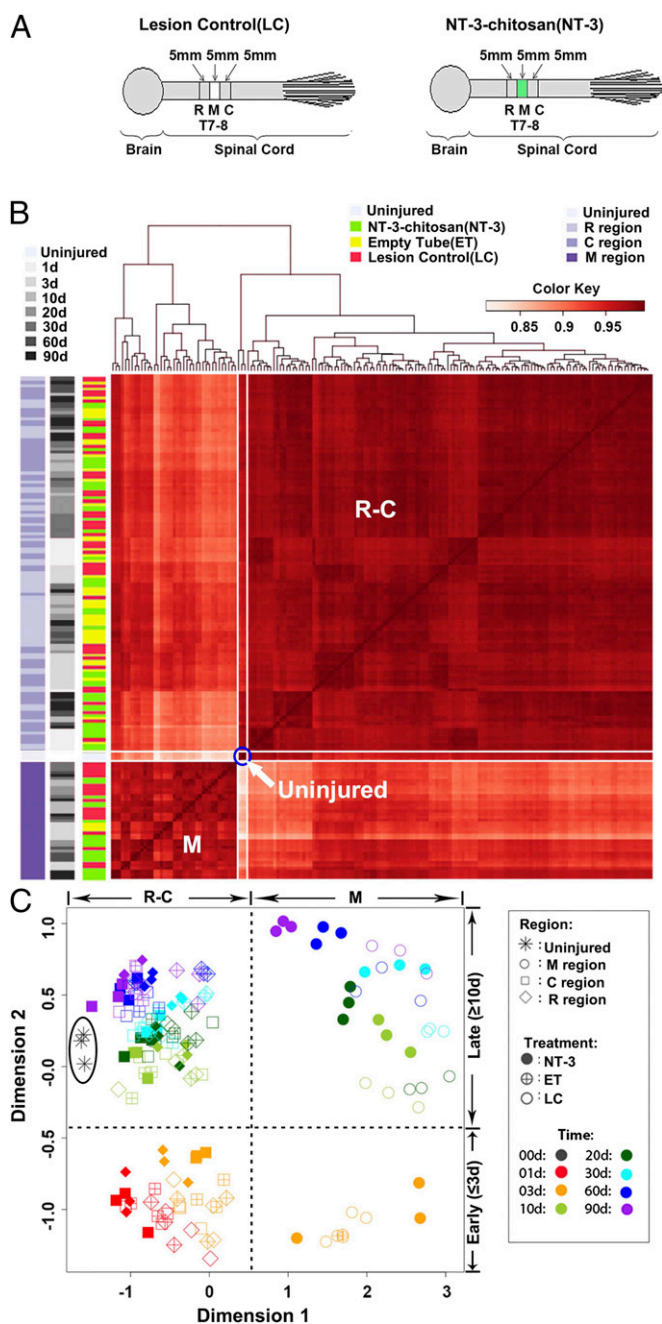
Fig. 1. Sample clustering revealed temporal and spatial changes following SCI with or without NT3-chitosan treatment. (*A*) A schema describing anatomic positions of spinal cord segments for the LC and NT3 samples used for transcriptome analyses. Empty chitosan tubes (ET) not loaded with NT3 were included as well. Since no tissues were grown inside the empty chitosan tubes except at one early time point (i.e., day 3 postsurgery), ET samples were mostly present in R and C groups. (*B*) Heat map of hierarchical clustering of pairwise correlations among all 167 samples. The side color bars represent sample coding. Sample correlations among three uninjured samples are indicated by a blue circle. White-framed regions represent correlations between uninjured samples and all other injury samples in the M region (below the blue circle, with bottom-most samples in darker colors, i.e., better correlations) and R and C regions (above the blue circle, also with bottom-most samples showing better correlations). Note that the vertical and horizontal frames are symmetrical. Bottom-most and left-most M region samples were enriched for NT-3-chitosan treatment groups. (*C*) PCA of all samples.

uniform measures of various perspectives of pathological events in the injured spinal cord will be hugely beneficial to SCI research

efforts. A cell can be generally defined by the set of genes that it expresses. Therefore the transcriptome reflects not only the identity of the cell, but also the physiological/pathological state of that cell. Presumably, within the injured spinal cord at different time points postinjury, various pathological cellular events could be reflected by transcription programs of injured spinal cord segments (8). Unfortunately, the lack of powerful bioinformatics data processing capability had confounded previous attempts of using transcriptome analyses to study SCI (8); however, a recently developed novel analytical approach, weighted gene-coexpression network analysis (WGCNA), now allows the identification of cores of gene networks based on a pairwise Pearson correlation matrix of all expressed genes across samples (12, 13). Genes with similar expression patterns across all samples will innately cluster together. These clustered cores, or modules, often represent genes involved in the execution of particular biological functions, including vasculature development, apoptosis, neuronal differentiation, and synaptic transmission, etc. Moreover, gene functions in particular cell types sometimes also cluster together, and thus some modules could be specific for oligodendrocytes/myelination, immune cells/defense response, neurons/synaptic transmission, and so forth. These events actually represent cell type-specific functions. The WGCNA method allows dissection of various ingredients (i.e., various pathological events) in the "soup" of an injured spinal cord via transcriptome analyses (14).

In the present study, we used WGCNA to establish gene module series representing major pathological events in a temporally and spatially specific manner following complete transection and extraction of the thoracic spinal cord, which can serve as objective outcome measurements. Using these measures, we further identified critical mechanisms underlying robust functional recovery by neurotrophin-3 (NT3)-chitosan after SCI.

Results

Experimental Design for Spinal Cord Transcriptome Analysis Post-SCI. In previous studies, we found that NT3-loaded chitosan biomaterial had a profound effect on promoting spinal cord regeneration as well as motor and sensory functional recovery (Fig. S1). To explore the molecular mechanisms by which NT3-chitosan facilitated spinal cord regeneration, we carried out extensive transcriptome analyses. Wistar female rats (200–220 g) were used for all experiments. Complete transection of the thoracic spinal cord at T7-8 was performed, with a 5-mm segment of the cord removed. The emptied space was either left alone [lesion control (LC)] or refilled with a 5-mm chitosan tube either loaded with NT3 or not loaded with NT3 [empty tube (ET)] before the dura was resutured. The success of the experiment was evaluated by parallel anatomical analysis at 90 d postsurgery demonstrating the growth of nerve-like bridging tissues within the NT3-chitosan tube, as well as behavioral analyses with a double-blind design indicating substantial functional recovery in the NT3-chitosan treatment group (Fig. S1).

Animals were euthanized at 1, 3, 10, 20, 30, 60, and 90 d postsurgery, and 5-mm segments of the spinal cord at the lesion site, as well as immediately caudal or rostral to the lesion segment, were collected and labeled with "R" for rostral, "C" for caudal, and "M" for lesion site (Fig. 1*A*). Spinal cord segments from four animals together were needed to provide sufficient RNA for microarray analyses as a single sample; thus, a total of 12 animals were euthanized to provide three samples at each time point. Quality mRNA was extracted, reverse-transcribed, and subjected to Affymetrix GeneChip (Rat Genome 230) 2.0 array analysis. Three uninjured spinal cord control samples corresponding to the lesion segment (5 mm) at T7-8 from 12 animals were included. Five reference RNA samples included in the microarray kit were used to control for a potential microarray batch effect.

Region-Specific Changes Following SCI Revealed by Sample Clustering. Unbiased hierarchical clustering of the complete dataset (167 samples from 668 animals) based on Pearson's correlation coefficient

of transcriptomes among pairs of samples in all combinations divided the samples into two major groups. All M region samples formed one cluster, and all R and C samples together formed the other large cluster (Fig. 1*B*). Three uninjured normal spinal cord samples clustered together (Fig. 1*B*, blue circle, white arrow) and were more closely correlated with R and C samples than with M samples, suggesting that more dramatic injury repair and tissue reconstitution events occurred within the M regions, whereas smaller changes occurred in R and C regions (Fig. 1*B*). In the figure, the white-framed stripes present information on correlations between the uninjured group and the rest of the samples; the darker the color, the better the correlation.

Sample clustering provided more information. For example, within the M region, NT3-chitosan–treated samples (labeled in green in Fig. 1*B*) tended to cluster together, and these samples correlated better with uninjured control samples than LC samples (labeled in red in Fig. 1*B*). Moreover, samples from the R and C regions that correlated best with uninjured control samples tended to be NT3-chitosan–treated samples and samples obtained at both early (day 1) and late (day 90) time points (Fig. 1*B*), suggesting that NT3-chitosan treatment had beneficial effects soon after injury and resulted in better recovery in the long run. Two-dimensional principal component analysis (PCA) of the whole data matrix further demonstrated that transcriptome differences caused by regional differences were greater than those caused by time differences, and those caused by time differences were greater than those caused by treatment differences (Fig. 1*C*). This suggests that (*i*) the M region underwent the most dramatic biological changes; (*ii*) different biological/pathological events occurred at different time points postinjury, which could be reflected in the transcriptome; and (*iii*) NT3-chitosan had beneficial effects, resulting in closer resemblance to uninjured cord, as indicated by the fact that most filled dots (NT3) were closer to uninjured samples compared with other treatment samples in the same region and at the same time (Fig. 1*C*).

Using WGCNA to Establish Gene Modules Underlying Pathological Events Post-SCI. Given that the M region underwent drastic tissue reconstitution starting with an empty space for both LC and NT3 groups (ET group was omitted as no tissue growth in the M region was observed), we expected that biological/pathological events occurring in R and C regions would be different from or less robust than those in the M regions, and thus should be analyzed separately. We first subjected uninjured/normal samples and all LC samples in R and C regions to WGCNA, with an emphasis on genes that underwent lesion-induced changes (a total of 7,500 annotated genes were included), which should digitally represent pathological cellular events in the lesion area after complete transection of the spinal cord. WGCNA identified 10 gene clusters/modules (designated as C1–C10) of coexpressed genes (Fig. 2 *A* and *B*).

Gene Ontology (GO) analysis of these 10 modules revealed several key biological processes that occurred in a temporally specific manner postinjury (Fig. 2*B* and Dataset S1). GO terms of each module revealed that synaptic transmission-related genes (C1), including neurotransmitter receptors, synaptic proteins, and ion channels (*Chrna7, Grm1, Syn2, and Kcnc1*), as well as axon/dendrite-related genes and calcium-signaling genes (*Amigo, Stxbp1, Map1b, Map2, Atp2b2, Camk2b, and Calm3*), underwent dramatic downregulation immediately after injury and remained low even at day 90 postsurgery, indicative of long-term impairment. Genes involved in sterol/cholesterol biosynthesis, tRNA metabolism, and ubiquitin-dependent protein degradation (C2) exhibited reduced expression with a slightly slower kinetics compared with C1, and also remained low throughout the 90-d period. In contrast, expression of genes involved in immune response, defense, inflammation, and cell death (C10: *Tlr4, Tgfb1, Vav1, C1qc, C1qb, and Casp1*) rose quickly after injury and remained high throughout the 90-d period, whereas expression of genes in another immune response (innate and adaptive)
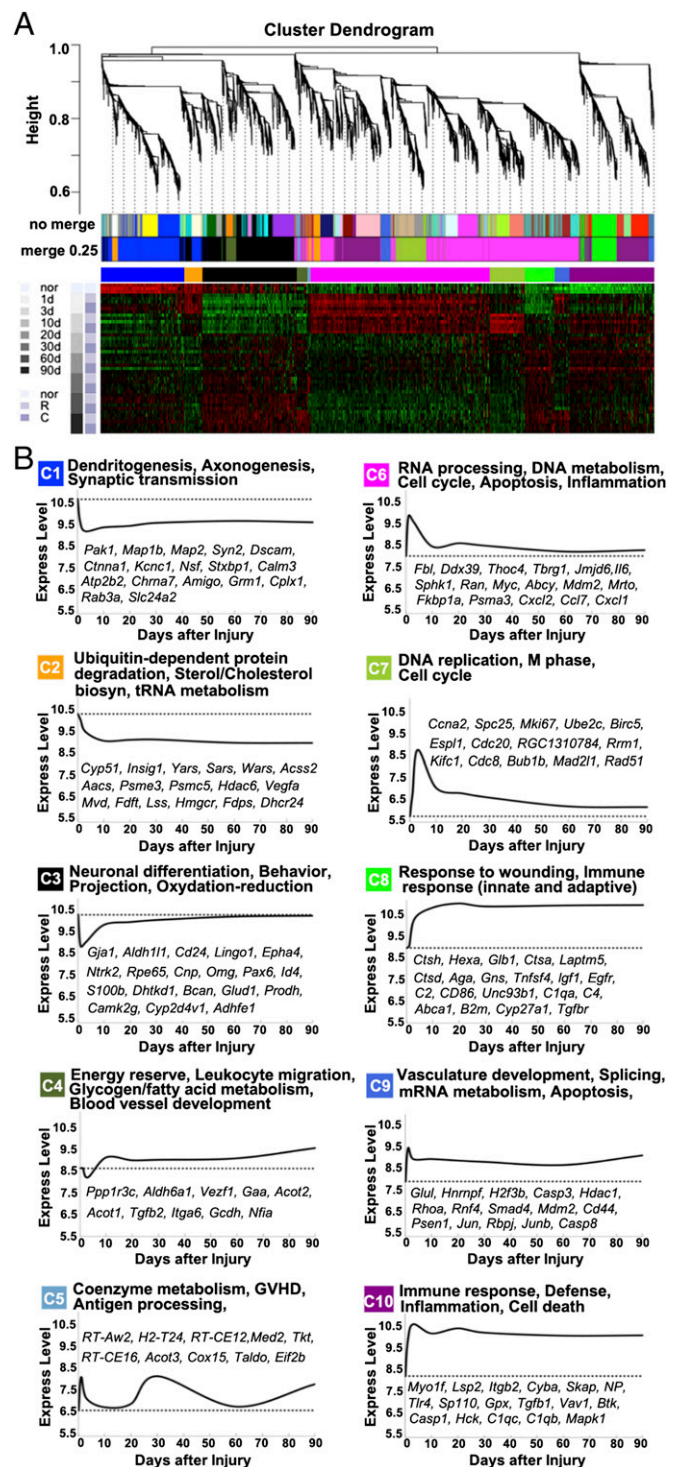

Fig. 2. WGCNA of LC samples in R and C regions identified gene modules underlying pathological events at different time points post-SCI. (*A*) Hierarchical cluster dendrogram of LC samples in R and C regions showing coexpression modules identified using WGCNA on the 7,500 most temporally regulated genes. Modules corresponding to branches are labeled with colors indicated by the color bands underneath the tree. With 0.25 threshold merging, 10 modules were generated. The heat map below shows gene expression of 10 modules of LC samples in R and C regions across all time points. (*B*) GO terms associated with each of the 10 modules, averaged expression levels of 30 genes with the highest module membership within each module at all time points for LC samples in R and C regions, and gene symbols of candidate genes within each module were shown.

Duan et al.

and wounding response module (C8: *Ctsh, Ctsd, Ctsa, Hexa, Cd86, Tnfsf4 Igf1, C2, C4, B2m,* and *Tgfbr*) increased slightly slower than those in C10, yet remained high for at least 90 d postinjury. In C3, a module related to neuronal differentiation and projection (*Gja1, Lingo1, Pax6, Epha4, Ntrk2, Rpe65,* and *CamK2g*), astrocyte and oligodendrocyte development (*Aldh1l1, Cd24, Cnp, Omg, Id4,* and *S100b*), and oxidation reduction (*Dhtkd1, Bcan, Glud1, Prodh,* and *Cyp2d4v1*), gene expression decreased immediately after injury but then reversed relatively quickly during the first 10 d post-SCI, and continued to slowly increase, reaching almost normal (uninjured) levels by day 90. This suggests that demyelination-remyelination and astrogliosis were dynamically regulated during the first 10-d period postinjury, and gradually diminished after 10 d. Likewise, C6 and C7, two modules related to cell cycle, apoptosis (*Fbl, Ddx39,* and *Thoc4*), and inflammation (*Il6, jmjd6,* and *Cxcl1/2/7*) rose quickly postinjury and then dropped rapidly over the first 10 d, and thereafter continued to gradually revert back to close to normal (uninjured) levels. C4 and C9, two modules related to metabolism of fatty acid, glycogen, mRNA and energy reserve, and vasculature development, also were dynamically regulated during the first 10 d and continued to increase slowly over the 90-d period. The unique module C5, involved in antigen processing and coenzyme metabolism, exhibited an "up-and-down" wavy time course. The biological significance of such changes remains to be elucidated.

Of note, as indicated by differential gene expression analyses, in LC samples, overall gene expression changes were not statistically significantly different in R regions versus C regions; only 0.2% of genes were differentially expressed in the two regions ($P < 0.01$). In contrast, in ET samples, 7% of the genes (i.e., 1,400 of 18,000) were differentially expressed in R versus C regions. These 1,400 genes were associated with cell adhesion, neuron projection, vasculature development, cell–cell signaling, and regulation of neurologic system processes, which appeared to be regulated more robustly in R regions. Considering that ET formed a physical barrier between R and C regions, since nothing grew in the chitosan-only tube, differential gene expression in R versus C regions suggested different injury signals were originated in the two regions. Under LC conditions, cellular components may shuttle between R and C regions, passing information back and forth to trigger similar injury responses, whereas such shuttling should be blocked in the ET group, resulting in different gene regulation in R versus C regions. In NT3 samples, approximately 518 of 18,000 genes were differentially expressed in R versus C regions, suggesting that NT3-chitosan connects the two regions, because cells did migrate into the tube. Moreover, NT3 appeared to elicit more robust changes in vasculature development, neuron development, and synaptic transmission in R regions than in C regions.

Taken together, our data indicate that WGCNA is capable of providing a digitized image of pathological events after complete spinal cord transection injury. Based on this information, outcome measurements could be established to evaluate various putative therapeutic interventions for SCI repair in a temporally and spatially specific manner.
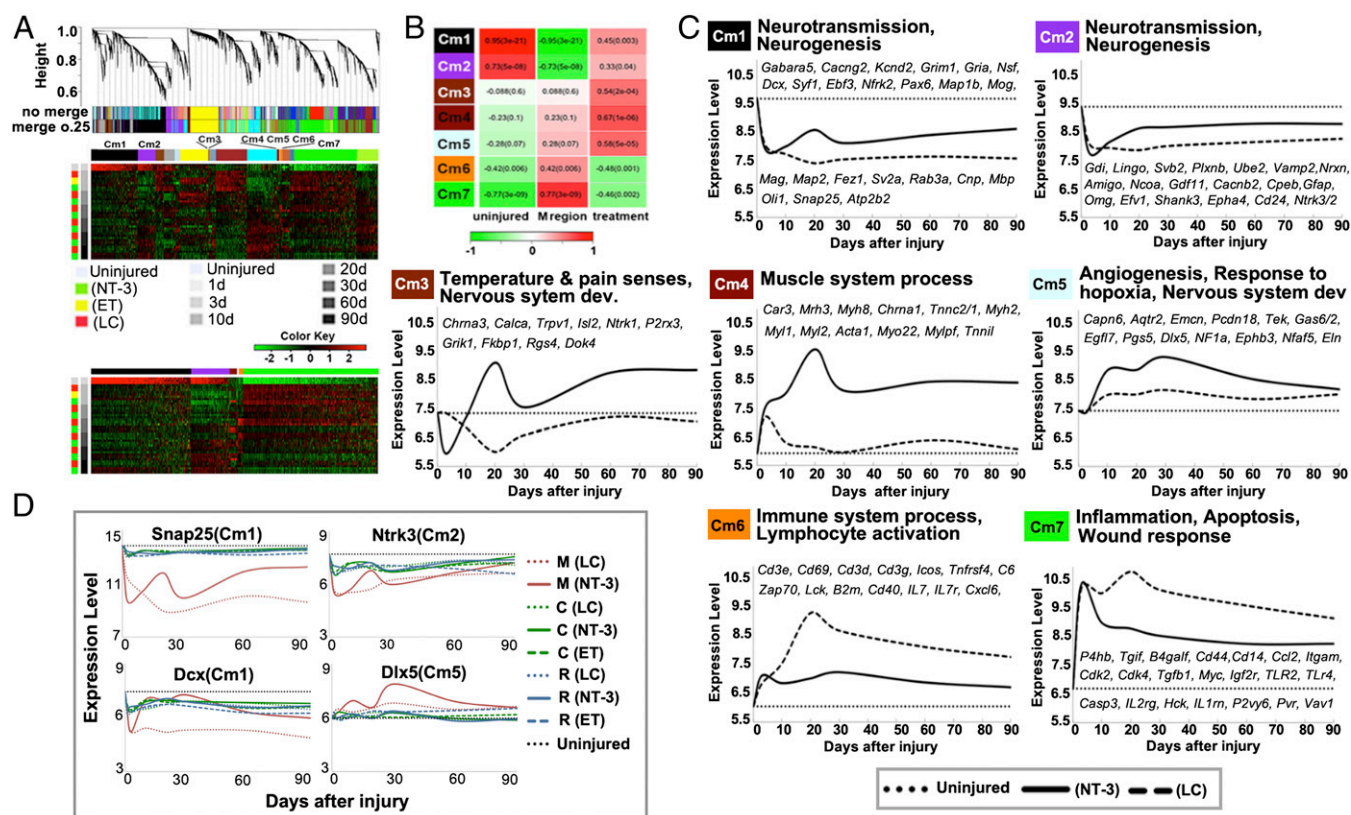
Fig. 3. WGCNA of uninjured and all M region injury samples uncovered molecular mechanisms underlying the proregeneration function of NT3-chitosan. (*A*) Hierarchical cluster dendrogram using WGCNA analyzing uninjured samples (N) and samples in the M regions. A total of 19 modules were identified after 0.25 threshold merging. Heat maps underneath demonstrated gene expression of all 19 modules or 7 selected modules across uninjured and all M region injury samples. (*B*) Module trait correlation analysis revealed that seven modules were significantly correlated with NT3-chitosan treatment. (*C*) GO terms of each of the seven modules, averaged gene expression of top 30 most NT3-chitosan regulated genes within each module, and lesion controls across all time points in the M region were shown. Candidate genes within each module were listed. (*D*) Gene expression of four candidate genes belonging to Cm1, Cm2, and Cm5 across all 167 samples (all regions, all treatments, all time points). Note the robust effect of NT3-chitosan in M regions.

NT3-Chitosan–Induced Regeneration Mediated by Antiinflammation and New Neurogenesis Following SCI. From PCA, it was apparent that gene regulation was more dynamic in the M region than in R and C regions, consistent with the fact that tissue reconstitution occurred in the M region. To strengthen the investigation to identify key cellular and molecular programs influenced primarily by NT3-chitosan, we carried out WGCNA on M region samples with noninjury controls. This analysis identified 19 modules (Fig. 3A), 7 of which showed statistically significant differences upon NT3-chitosan treatment (Fig. 3B). Analysis of the module–trait relationship identified five modules (Cm1, Cm2, Cm3, Cm4, and Cm5) as positively correlated with NT3-chitosan treatment and two modules (Cm6 and Cm7) as negatively correlated with NT3-chitosan treatment ($P < 0.05$) (Fig. 3B).

GO and hub gene network analyses, shown in Fig. S2 and Dataset S2, indicated that Cm1 and Cm2 were related to neurogenesis; Cm4 was related to muscle contraction; Cm3 was related to pain and temperature sensory processing; Cm5 was related to angiogenesis, response to oxygen levels, and nervous system development; Cm6 was related to immune response; and Cm7 was related to response to wounding, stress, and inflammation. The averaged gene expression of each module further indicated that NT3-chitosan enhanced vascularization (blood supply), which was required for proper tissue repair. NT3-chitosan also clearly suppressed inflammatory responses (Cm6 and Cm7), which were classically considered key to attenuating secondary lesions after SCI. Therefore, the antiinflammatory effect elicited by NT3-chitosan also could contribute to the better regeneration outcome.

One exciting finding was the enhanced expression of modules Cm1 and Cm2 (related to neurogenesis and neurotransmission) in response to NT3-chitosan. Moreover, Cm3 and Cm5 also contained many neurogenesis genes, including *Dlx5, Isl2, Trpv1, Chrna3, Ntrk1, Ngfr, Agrn*, GDNF receptors, *Nrep, Smo, and Gata2*. Although NT3-chitosan enhanced gene expression in Cm1 and Cm 2 and in Cm3 and Cm5, these four modules behaved differently. Cm1/2 represented genes related to neuronal differentiation, which were expressed at high levels in uninjured/normal spinal cord, whereas Cm3/5 represented neuronal differentiation genes, which were not highly expressed in normal adult spinal cord but were elicited de novo by NT3-chitosan. Interestingly, a muscle contraction module (Cm4) also was heavily induced by NT3-chitosan in the M region. This finding was unexpected and merited further investigation to determine the contribution of this module to better functional recovery after SCI. Expression levels of candidate genes from Cm1 (*Dcx* and *Snap25*), Cm2 (*Ntrk3*), and Cm5 (*Dlx5*) across all samples (all regions and all times) demonstrated robust regulation of these genes by NT3-chitosan in the M region compared with R and C regions (Fig. 3D). Expression plots for additional genes involved in NSC differentiation are shown in Fig. S3.

Taken together, our data from transcriptome WGCNA indicated that NT3-chitosan served primarily to enhance vascularization and suppress inflammatory immune responses, establishing an optimal microenvironment to support endogenous NSCs to differentiate into new neurons, which subsequently formed nascent local neural networks to participate in regeneration after SCI (15).

Biological Confirmation. To assess whether NT3-chitosan indeed served as an antiinflammatory agent in our experiments, we stained injured spinal cord with NT3-chitosan treatment or no treatment using an anti-CD45 antibody, which labeled all infiltrating leukocytes (Fig. 4 A and B), and found reduced leukocyte infiltration in the NT3-chitosan group. To examine whether it was the chitosan material or NT3 per se, or the two together that elicited the maximum anti-inflammatory effect, we measured inflammatory cytokines from a mouse macrophage RAW cell line cocultured with lipopolysaccharide (LPS; positive control), chitosan, soluble NT3, and NT3-conjugated chitosan (NT3-chitosan). Our results demonstrated that at 1 d and 3 d after treatment,

IL-1α/β, IL-6, NF-kb, and TGF-β expression and secretion were increased with LPS treatment, little changed with chitosan only or soluble NT3 treatment, but significantly decreased with NT3-chitosan treatment, suggesting that NT3-loaded chitosan could significantly suppress inflammatory cytokine production from RAW cells (Fig. 4C).

Moreover, we found that when RAW cells were cocultured with rat spinal cord slices, the aforementioned inflammatory cytokine secretion was increased as well, which could be suppressed by NT3-chisosan, and that NT3 antibody could block the effect of NT3-chitosan. Of note, we observed the same phenomenon when measuring mouse-specific cytokines (generated from RAW cells) or rat-specific cytokines (generated from rat spinal cord slices) (Fig. 4 C and D and Fig. S4).

To obtain evidence to support the notion that antiinflammation was beneficial for functional recovery following SCI, we compared functional recovery using the Basso Mouse Scale (BMS) scoring system in a double-blinded manner on spinal cord crush-injured wild type and immunocompromised SCID mice. The SCID mice clearly demonstrated better functional recovery post-SCI (Fig. 4E). Finally, staining of injured spinal cords at the lesion site in the LC and NT3-chitosan groups revealed robust neural filament (NF) staining only in the NT3-chitosan–treated samples. Numerous
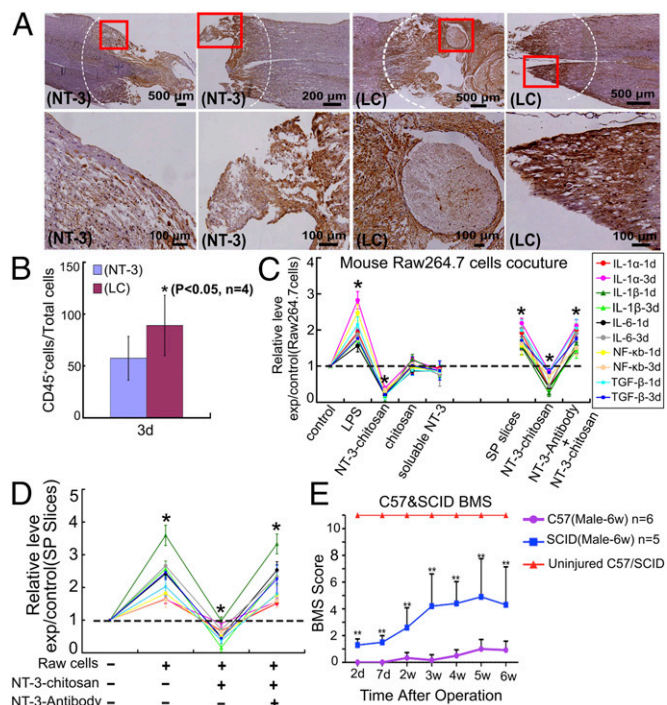

Fig. 4. NT3 chitosan creates a reduced inflammatory environment, which is beneficial for functional recovery post-SCI. (A and B) CD45 staining to label inflammatory leukocytes in injured rat spinal cord sections for both NT3 and LC groups and quantitative analyses of CD45$^+$ cells over total cells, within injured nerve tips demarcated by the dotted prentices. Red boxes indicate regions that are magnified in the lower panels. Note the reduced CD45 immunoreactivity with NT3-chitosan treatment. (C) qPCR of mouse inflammatory cytokines from mouse RAW264.7 cells cocultured for 1 d and 3 d with LPS, chitosan, soluble NT3, and NT3-chitosan, as well as rat spinal cord slices with or without NT3-chitosan or neutralizing antibody against NT3. Note that NT3 was crucial (because an antibody could block the effect), but only NT3-chitosan could significantly reduce the generation of inflammatory cytokines. (D) qPCR of rat inflammatory cytokines released from rat spinal cord slices cocultured with RAW264.7 cells, with or without NT3-chitosan or antibody against NT3. Cytokine color labeling is the same as in C. (E) BMS scores of C57 black 6 and SCID mice after crush injury of the spinal cord at T7-8 up to 6 wk after injury. All data are presented as mean ± SD; $n \geq 4$. $P < 0.05$, one-way ANOVA with Bonferroni post hoc analysis.

NF$^+$ cells were present in the NT3-chitosan tube, suggesting the addition of new neuronal components in the biomaterial, consistent with the transcriptome analyses. More detailed analyses were described in same issue (15), addressing the role of NT3-chitosan in the promotion of new neurogenesis, formation of a nascent local neural network, and subsequent connection to ascending and descending nerve fibers, leading to functional recovery.

Discussion

In this study, we used unbiased objective analyses of the transcriptomes of injured spinal cord segments to reveal important underlying molecular programs that were altered in a temporally and spatially specific manner after complete SCI. This analysis identified quantifiable changes in various gene programs representing distinct biological/pathological processes postinjury, which could be regulated individually or in combination by various interventions. Specifically, we revealed that NT3-chitosan enhanced vascularization and suppressed inflammatory immune responses, providing an optimal environment for endogenous NSCs (likely including CD133$^+$ ependymal cells and their downstream lineage cells) to generate newly born neurons, forming a nascent neural synaptic network, which served as an information relay station to reconnect ascending and descending sensory and motor information, achieving functional recovery (16).

This mechanistic insight was further substantiated by the observation that NT3-chitosan elicited strong antiinflammatory effects in vitro and in vivo using classical biochemical measures and immunohistochemistry analyses. Moreover, these analyses revealed that a failure in generating new neurons from endogenous NSCs, due to the harsh inflammatory environment, could be a major obstacle to proper regeneration and functional recovery after SCI (15). One underlying premise for WGCNA is that genes functioning together are regulated together. This premise likely explains why WGCNA is a very powerful analysis for revealing molecular gene networks underlying biological functions (12–14). In addition to gene modules, the hub gene network analyses also revealed potential key regulatory factors (hub genes, with the greatest module membership and connectivity), which potentially could serve as therapeutic targets to alter specific gene programs following SCI. Once expression of gene modules can be used to quantitatively represent the various pathological events, these sets of new criteria can be used in outcome measurement of various potential therapeutic interventions. In addition, these potential biomarkers can be used to evaluate the severity of SCI. With such useful tools, rational designs of combinatorial therapies, for example, those that aimed at promoting neurogenesis and those aimed at suppressing inflammatory immune responses, could be applied

and evaluated. In addition, if correlations can be established between the transcriptome of the injured spinal cord and that of the peripheral blood, new sets of biomarkers for molecular diagnostics, as well as outcome measurements of SCI and potential treatment, can be established, which will greatly benefit future SCI research and therapeutic development.

Materials and Methods

Animal Surgery. All animal procedures were carried out in accordance with the guidelines from the Capital Medical University Institutional Animal Care and Use Committee. Wistar rats weighing 200–220 g were used for the rat complete transection SCI study. In addition, 6- to 8-wk-old C57 and SCID male mice were subjected to spinal cord crush injury. Details are provided in SI Materials and Methods.

Behavioral Analyses. Before the operation and at 1 d postsurgery and each week thereafter, observers who were blinded to the treatment methods and groups applied Basso–Beattie–Bresnahan (BBB) scoring in an open field to evaluate hindlimb locomotor function (10, 17). BMS was used for mouse analyses.

Microarray Analyses. These analyses are described in detail in SI Materials and Methods.

WGCNA. Both MN datasets (42 samples, including M region injury data and normal/uninjured controls) and RCN-LC datasets (45 samples, including R and C region lesion control/LC samples together with normal/uninjured controls) were independently constructed for WGCNA (18, 19). Details are provided in SI Materials and Methods.

Quantitative PCR and ELISA Analyses. These analyses are described in SI Materials and Methods.

RAW Cell Culture and Coculture with Rat Spinal Cord Slices. Mouse microphage RAW264.7 cells were used to evaluate the antiinflammatory effects of NT3-chitosan. Details are provided in SI Materials and Methods.

1. Facchiano F, et al. (2002) Promotion of regeneration of corticospinal tract axons in rats with recombinant vascular endothelial growth factor alone and combined with adenovirus coding for this factor. *J Neurosurg* 97(1):161–168.
2. Lang BT, et al. (2015) Modulation of the proteoglycan receptor PTPσ promotes recovery after spinal cord injury. *Nature* 518(7539):404–408.
3. Hirschberg DL, Schwartz M (1995) Macrophage recruitment to acutely injured central nervous system is inhibited by a resident factor: A basis for an immune-brain barrier. *J Neuroimmunol* 61(1):89–96.
4. Liu K, et al. (2010) PTEN deletion enhances the regenerative ability of adult corticospinal neurons. *Nat Neurosci* 13(9):1075–1081.
5. Cummings BJ, et al. (2005) Human neural stem cells differentiate and promote locomotor recovery in spinal cord-injured mice. *Proc Natl Acad Sci USA* 102(39):14069–14074.
6. Keirstead HS, et al. (2005) Human embryonic stem cell-derived oligodendrocyte progenitor cell transplants remyelinate and restore locomotion after spinal cord injury. *J Neurosci* 25(19):4694–4705.
7. Courtine G, et al. (2008) Recovery of supraspinal control of stepping via indirect propriospinal relay connections after spinal cord injury. *Nat Med* 14(1):69–74.
8. Aimone JB, Leasure JL, Perreau VM, Thallmair M; Christopher Reeve Paralysis Foundation Research Consortium (2004) Spatial and temporal gene expression profiling of the contused rat spinal cord. *Exp Neurol* 189(2):204–221.
9. Profyris C, et al. (2004) Degenerative and regenerative mechanisms governing spinal cord injury. *Neurobiol Dis* 15(3):415–436.
10. Li X, Yang Z, Zhang A, Wang T, Chen W (2009) Repair of thoracic spinal cord injury by chitosan tube implantation in adult rats. *Biomaterials* 30(6):1121–1132.
11. Li XG, Yang ZY, Yang Y (2006) Morphological and electrophysiological evidence for regeneration of transected spinal cord fibers and restoration of motor functions in adult rats. *Chin Sci Bull* 51(8):918–926.
12. Zhang B, Horvath S (2005) A general framework for weighted gene co-expression network analysis. *Stat Appl Genet Mol Biol* 4(1):e17.
13. Langfelder P, Horvath S (2008) WGCNA: An R package for weighted correlation network analysis. *BMC Bioinformatics* 9:559.
14. Oldham MC, et al. (2008) Functional organization of the transcriptome in human brain. *Nat Neurosci* 11(11):1271–1282.
15. Yang Z, et al. (2015) NT-3-chitosan elicits robust endogenous neurogenesis to enable functional recovery after spinal cord injury. *Proc Natl Acad Sci USA* 112: 13354–13359.
16. Luo Y, et al. (2015) Single-cell transcriptome analyses reveal signals to activate dormant neural stem cells. *Cell* 161(5):1175–1186.
17. Basso DM, Beattie MS, Bresnahan JC (1995) A sensitive and reliable locomotor rating scale for open field testing in rats. *J Neurotrauma* 12(1):1–21.
18. Yip AM, Horvath S (2007) Gene network interconnectedness and the generalized topological overlap measure. *BMC Bioinformatics* 8:22.
19. Horvath S, Dong J (2008) Geometric interpretation of gene coexpression network analysis. *PLOS Comput Biol* 4(8):e1000117.
20. Huang W, Sherman BT, Lempicki RA (2009) Systematic and integrative analysis of large gene lists using DAVID bioinformatics resources. *Nat Protoc* 4(1):44–57.
21. Li X, Yang Z, Zhang A (2009) The effect of neurotrophin-3/chitosan carriers on the proliferation and differentiation of neural stem cells. *Biomaterials* 30(28):4978–4985.

NEUROSCIENCE